

# Flutter Part 1: Fundamentals with quasi-steady aerodynamic theory

Sina Stapelfeldt \*

Imperial College London  
von Karman Institute for Fluid Dynamics

18 August 2022

## Contents

<b>1</b>	<b>Introduction</b>	<b>3</b>
<b>2</b>	<b>Aeroelastic formulation</b>	<b>5</b>
2.1	Typical section . . . . .	5
2.2	Equation of motion . . . . .	6
2.3	Non-dimensionalisation . . . . .	8
2.4	Steady aerodynamic forces . . . . .	9
2.5	Quasi-steady behaviour . . . . .	9
<b>3</b>	<b>Coupled bending-torsion flutter</b>	<b>11</b>
<b>4</b>	<b>Parameter dependency</b>	<b>15</b>
4.1	Mass ratio . . . . .	15
4.2	Frequency ratio . . . . .	15
4.3	Location of centre of mass and torsional axis . . . . .	15
<b>5</b>	<b>Conclusions</b>	<b>19</b>

---

\*The author would like to thank Roger Ziepke-Sonntag for his contribution to these lecture notes, in particular for proofreading, spotting mistakes in the equations and generally improving readability.



# 1 Introduction

Flutter is a dynamic instability caused by the interaction of aerodynamic, elastic and inertial forces. It therefore belongs to the class of dynamic aeroelastic phenomena, others being buffeting or gust response, and sits in the centre of Collar's famous triangle of forces illustrated in Figure 1. Flutter causes uncontrolled vibration with rising amplitude, and when the stress in the material exceeds steady or fatigue limits, it can ultimately lead to the destruction of the structure. Unlike gust response or buffeting, flutter does not require any external forces. It is the result of a positive feedback mechanisms between deformation of the structure and resulting unsteady aerodynamic loads. It is commonly encountered in lifting surfaces, such as aircraft wings, tails and control surfaces and also in wind turbine blades, rotor craft, turbomachinery blades, or even bridges. Famous examples of flutter are the first recorded flutter event of the Handley Page airplane in 1916 and the collapse of the Tacoma Narrows Bridge in 1940. Because of the potentially catastrophic consequences, flutter must in general be completely eliminated by design or at least prevented from occurring within the flight envelope. A historical review of flutter research is given, for example, by Garrick and Reed III (1981).

To design against flutter, the stiffness or mass distributions of the structure or its aerodynamics have to be changed. This tends to result in structures which are heavier than designs optimised for aerodynamic performance (the so-called aeroelastic penalty). This is still a concern in modern engineering and a lot of research is dedicated to the improvement of modelling and detection capabilities to design flutter-free structures, develop mitigation measures or implement automatic control measures. While most of the early research on flutter was performed in wind tunnels or using analytical models, modern techniques employ high-fidelity models of structural dynamics and aerodynamics to analyse the stability of complex structures such as whole aircraft or multi-stage aero-engine compressors. Often, neither the mechanical properties nor the aerodynamics of such complex systems are completely understood or accurately modelled, and therefore experimental testing remains a vital part of the development process.

Although flutter is a complex phenomenon, the nature of flutter and its analysis technique can be understood from the coupled structural and aerodynamic analysis of a simplified two-dimensional model. This lecture will introduce such a model, the governing equation and its stability analysis. The behaviour of the two-dimensional model is described by a linear set of structural dynamic equations which are coupled with a linear representation of the aerodynamic forces resulting from the structural deformations. In this lecture, the aerodynamic analysis is restricted to steady forces, which presents a significant limitation. When linear models for the unsteady aerodynamics are included, the analysis is typically referred to as *classical flutter analysis*. In reality both structural

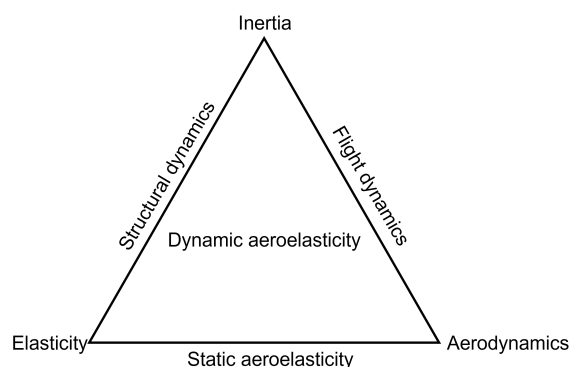


Figure 1: Collar's triangle of forces

dynamics and aerodynamics give rise to non-linear effects. The flow over the surface may separate for part or all of the vibration cycle, leading to so-called *stall flutter*. Large deflections, mechanical contacts or control systems may also introduce non-linearities.

Typical flutter analysis concentrates on the stability of infinitesimal small deflections, since it is undesirable for any system to be unstable when imposed to small random perturbations. Often, the introduction of non-linearities at larger deflections actually stabilises the system. This is the case, for example, in stall flutter when flow separation limits the amplitudes and leads to periodic limit-cycle oscillations.

A discussion of unsteady forces and non-linearities is out of scope of this lecture, but some methods for analysis with unsteady aerodynamics and non-linear effects will be introduced in Part 2. The simplified treatment presented in the following is chosen to demonstrate important characteristics of flutter instability and illustrate flutter analysis.

## 2 Aeroelastic formulation

### 2.1 Typical section

A ‘typical section model’, which represents the cross section of a wing or rotor blade will be used to demonstrate the stability analysis. This model has historically been used to perform flutter analyses. It is an extremely simplified case which still shares many properties with the more complex systems found across engineering applications. The model and nomenclature here follows closely those of Hodges and Pierce (2011). A similar, more general analysis can be found in Bisplinghoff et al. (2013).

A schematic of the typical two-dimensional section model is shown in Fig. 2. The aerofoil section is elastically mounted on a set of discrete springs. In the standard case shown here with two degrees of freedom, these are a compression and a torsional spring representing the structural bending and torsional stiffness of the three-dimensional wing. The corresponding two degrees of freedom are plunging and twisting, denoted by  $h$  and  $\theta$ . The spring stiffness constants are accordingly labelled  $k_h$  and  $k_\theta$ . The springs are mounted on the reference point labelled  $x_R$ . The chord length is denoted by  $c$  but it is common to use semi-chord  $b = c/2$  as a reference length.

Two more points of interest are the point where the aerodynamic forces are acting on and the centre of mass  $x_{CM}$ . To simplify the aerodynamic analysis, we will consider the aerodynamic forces acting through the aerodynamic centre  $x_{AC}$ . The offset between the centre of mass and the reference point is defined as  $x_R - x_{CM} = b(e - a) = bx_\theta$ . The incoming air is axial, such that the instantaneous incidence angle is equal to  $\theta$ . This assumption is made for simplicity of the expressions in this example but it does not impact the generality of the results since flutter stability concerns dynamic deviations from a given steady-state. In a real case, the wing would be at an angle of attack and  $\theta$  would represent the deviation from this angle. The generalized aerodynamic forces acting in the two degrees of freedom are given by

$$F_h = -L \quad (1)$$

$$F_\theta = M_{AC} + (x_R - x_{AC})L = M_{AC} + b\left(\frac{1}{2} + a\right)L \quad (2)$$

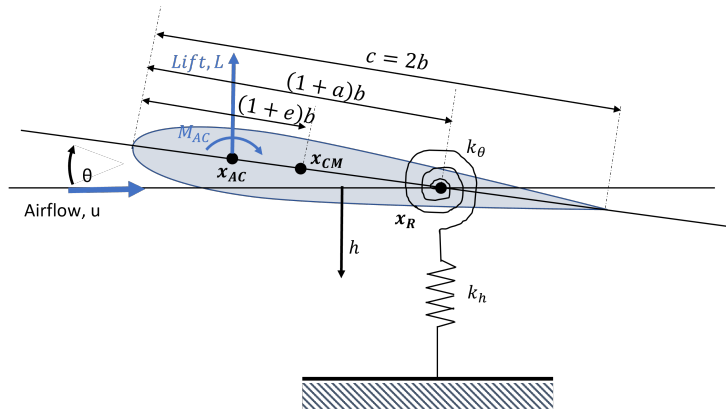


Figure 2: Typical section model

where  $M_{AC}$  is the moment about the aerodynamic centre. The second line is the moment acting on the centre of torsion. It is here referred to as a generalized force, i.e. a force acting in the direction of the coordinate  $\theta$ , to keep the notation general. In classical flutter, the lift and moment can be considered linear functions of the deformation (and their derivatives), i.e.  $L = (dC_L/d\theta)\theta$ , where the lift curve slope  $dC_L/d\theta$  is constant in  $\theta$ . Assuming steady flow and thin airfoil theory, they can be simplified significantly since  $L = 2\pi\rho U^2 b\theta$  and  $M_{AC} = 0$ .

## 2.2 Equation of motion

The equation of motion for this system for the plunge and twist degree of freedom is given by Eq. 3. For a derivation, the reader is referred to Hodges and Pierce (2011).

$$\begin{bmatrix} m & mbx_\theta \\ mbx_\theta & I_\theta \end{bmatrix} \begin{bmatrix} \ddot{h} \\ \ddot{\theta} \end{bmatrix} + \begin{bmatrix} k_h & 0 \\ 0 & k_\theta \end{bmatrix} \begin{bmatrix} h \\ \theta \end{bmatrix} = \begin{bmatrix} F_h \\ F_\theta \end{bmatrix} \quad (3)$$

where  $I_\theta = I_{CM} + mb^2x_\theta^2$  and  $I_{CM}$  is the moment of inertia about the centre of mass. The mass matrix includes off-diagonal terms  $mbx_\theta$  crossed by inertial coupling of the plunging and twisting motion. Because the centre of mass is located ahead of the torsional axis, a vertical downward acceleration  $\ddot{h}$  is accompanied by an inertial force  $m\ddot{h}$  acting in the upward direction through the centre of mass, which produces a positive moment about the centre of gravity  $mbx_\theta\ddot{h}$ . Similarly, an angular acceleration  $\ddot{\theta}$  around the centre of torsion  $x_R$  creates a linear acceleration of  $mbx_\theta\ddot{\theta}$  at the centre of gravity, resulting in a symmetric mass matrix. The stiffness matrix is diagonal because the elastic forces are decoupled. The aerodynamic forces on the right hand side are the generalized forces acting in the two degrees of freedom, in this case lift and moment. They are more complicated and depending on their exact nature introduce further coupling between the two degrees of freedom, which will be seen later.

We will now make a few substitutions and manipulate the equations to arrive in a form which is more suitable for analysis. This follows the procedure in Hodges and Pierce (2011). Firstly, the structural stiffness will be expressed in terms of the natural frequencies of the in-vacuo system  $\omega_h = \sqrt{k_h/m}$  and  $\omega_\theta = \sqrt{k_\theta/I_\theta}$ . (These can be obtained by setting the right hand side of Eq. 3 to zero.) Secondly, we change the plunge variable to  $h/b$  and multiple the first equation by  $b$ .

$$\begin{bmatrix} mb^2 & mb^2x_\theta \\ mb^2x_\theta & I_\theta \end{bmatrix} \begin{bmatrix} \ddot{h}/b \\ \ddot{\theta} \end{bmatrix} + \begin{bmatrix} mb^2\omega_h^2 & 0 \\ 0 & I_\theta\omega_\theta^2 \end{bmatrix} \begin{bmatrix} h/b \\ \theta \end{bmatrix} = \begin{bmatrix} bF_h \\ F_\theta \end{bmatrix} \quad (4)$$

Now, all the terms have the same units. As already mentioned, in classical flutter it is assumed that the aerodynamic forces are linear functions of the the plunging and twisting displacements and velocities:  $F_h = f(h/b, \dot{h}/b, \theta, \dot{\theta})$ ,  $F_\theta = g(h/b, \dot{h}/b, \theta, \dot{\theta})$ . Expressing this relationship with complex coefficients,  $F_h = \tilde{F}_{hh}h/b + \tilde{F}_{h\theta}\theta$  and  $F_\theta = \tilde{F}_{\theta h}h/b + \tilde{F}_{\theta\theta}\theta$ , they can be further categorised into four components:

- $\tilde{F}_{hh}$  = Plunging force due to plunging motion
- $\tilde{F}_{h\theta}$  = Plunging force due to twisting motion
- $\tilde{F}_{\theta h}$  = Twisting force due to plunging motion
- $\tilde{F}_{\theta\theta}$  = Twisting force due to twisting motion

These force coefficients  $\tilde{F}$ , also known as *aerodynamic influence coefficients*, can be interpreted as the unsteady aerodynamic force resulting from a unit deflection in the generalised displacements  $h/b$  or  $\theta$ . They are complex and the real part represents the component in phase with the displacement, while the imaginary part represents the component in phase with the velocity.

Substituting the expressions for the aerodynamic forces into Eq. 4, the equation of motion becomes:

$$\begin{bmatrix} mb^2 & mb^2 x_\theta \\ mb^2 x_\theta & I_\theta \end{bmatrix} \begin{bmatrix} \ddot{h}/b \\ \ddot{\theta} \end{bmatrix} + \begin{bmatrix} mb^2 \omega_h^2 & 0 \\ 0 & I_\theta \omega_\theta^2 \end{bmatrix} \begin{bmatrix} h/b \\ \theta \end{bmatrix} = \begin{bmatrix} b\tilde{F}_{hh} & b\tilde{F}_{h\theta} \\ \tilde{F}_{\theta h} & \tilde{F}_{\theta\theta} \end{bmatrix} \begin{bmatrix} h/b \\ \theta \end{bmatrix} \quad (5)$$

In this case, Eq. 5 is a set of linear ordinary differential equations which has general solutions which are exponential functions of time:

$$h(t) = \tilde{h}e^{\lambda t} \quad \theta(t) = \tilde{\theta}e^{\lambda t} \quad (6)$$

where  $\tilde{h}$  and  $\tilde{\theta}$  are complex amplitudes. Their real parts represent the vibration amplitudes and their relative phases represent the phase shift between the plunging and twisting motion, i.e. the mode shape.

To keep the notation concise, we introduce the mass  $M$ , stiffness  $K$  and aerodynamic matrices  $F$  and the generalised displacement vector  $q = [h/b \quad \theta]^T = \tilde{q}e^{\lambda t}$ :

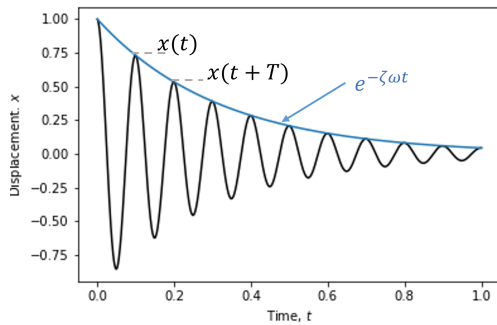
$$M\ddot{q} - [K - F]q = 0 \quad (7)$$

Making the substitution  $q = \tilde{q}e^{\lambda t}$ , Eq. 7 transforms into an eigenvalue problem:

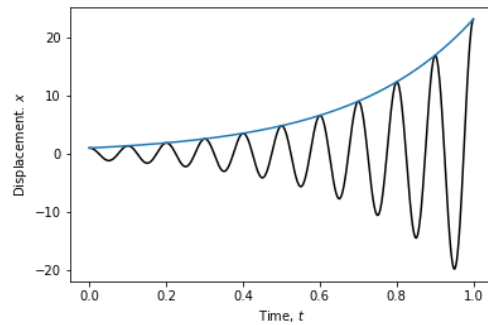
$$\lambda^2 I - M^{-1}[K - F] = 0 \quad (8)$$

The roots are typically two complex conjugate pairs describing two vibration modes, for example:

$$\lambda_1 = \Gamma_1 \pm i\Omega_1 \quad \lambda_2 = \Gamma_2 \pm i\Omega_2 \quad (9)$$



(3.1)  $\zeta = 0.05$



(3.2)  $\zeta = -0.05$

Figure 3: Time histories for stable, and unstable system where  $\omega$  is the vibration frequency and  $T = 2\pi/\omega$  is the vibration period.

By analogy to a spring-damper system ( $\ddot{x} + 2\zeta\omega\dot{x} + \omega^2x = 0$ ), the complex eigenvalues relate to the critical damping ratio  $\zeta = -\Gamma/\omega$  and natural frequency of the coupled aeroelastic system  $\omega = \Omega/\sqrt{1 - \zeta^2}$ . Typical responses for different values of  $\Gamma$  are shown in Fig. 3.

Looking at Eq. 7, it is possible to split the aerodynamic forces into real and imaginary components when moving them to the left hand side. This is done by considering that  $Fq = [\Re(F) + i\Im(F)]q = \Re(F)q + i\Im(F)\frac{\dot{q}}{\lambda}$  since  $q = \tilde{q}e^{\lambda t}$  and  $\dot{q} = \tilde{q}\lambda e^{\lambda t} = \lambda q$ .

$$M\ddot{q} - [\Im(F)/\lambda]\dot{q} + [K - \Re(F)]q = 0 \quad (10)$$

In this form, it is clear that the aerodynamic forces introduce damping and modify the effective stiffness of the system.

The last steps (from Eq. 7 apply to any aeroelastic system which can be modelled in terms of a set of generalized displacements, not just the typical section.

### 2.3 Non-dimensionalisation

Equation 5 can be solved as written. However, to understand the nature and characteristics of flutter it is more informative to express it in terms of non-dimensional variables. The aerodynamic forces on the right hand side are functions of the aerodynamic (lift and moment) coefficients and can be written as:

$$\begin{aligned} \tilde{F}_{hh} &= \tilde{C}_{hh}\rho u^2 b \\ \tilde{F}_{h\theta} &= \tilde{C}_{h\theta}\rho u^2 b \\ \tilde{F}_{\theta h} &= \tilde{C}_{\theta h}\rho u^2 b^2 \\ \tilde{F}_{\theta\theta} &= \tilde{C}_{\theta\theta}\rho u^2 b^2 \end{aligned} \quad (11)$$

Substituting this into Eq. 5, manipulating the equations and identifying the non-dimensional parameters:

$$\begin{aligned} \text{Mass ratio:} & \mu = m/(\rho\pi b^2) \\ \text{Frequency ratio:} & \sigma = \omega_h/\omega_\theta \\ \text{Radius of gyration:} & r = \sqrt{I_\theta/(mb^2)} \\ \text{Reduced velocity:} & V = u/(b\omega_\theta) \end{aligned} \quad (12)$$

where  $m$  is the mass per unit span. The origin of the  $\pi$  in the definition of mass ratio lies in thin airfoil theory, and the mass ratio can thus be interpreted as the ratio of the mass of the blade to the mass of air in a circle with radius semi-chord.

Eq. 5 can be rewritten as:

$$\frac{1}{V^2\omega_\theta^2} \begin{bmatrix} 1 & x_\theta \\ x_\theta & r^2 \end{bmatrix} \begin{bmatrix} \ddot{h}/b \\ \ddot{\theta} \end{bmatrix} + \begin{bmatrix} \sigma/V^2 & 0 \\ 0 & r^2/V^2 \end{bmatrix} \begin{bmatrix} h/b \\ \theta \end{bmatrix} = \frac{1}{\mu} \begin{bmatrix} \tilde{C}_{hh} & \tilde{C}_{h\theta} \\ \tilde{C}_{\theta h} & \tilde{C}_{\theta\theta} \end{bmatrix} \begin{bmatrix} h/b \\ \theta \end{bmatrix} \quad (13)$$

Eq. 13 is the non-dimensional equation of motion for a typical aerofoil section in plunging and twisting motion. This is an eigenvalue problem in terms of a new non-dimensional eigenvalue, historically referred to as  $p = \lambda b/u$ :



$$p^2 I - [M^*]^{-1} [K^* - F^*] = 0 \quad (14)$$

where the  $*$  denotes the non-dimensional form of the mass, stiffness and aerodynamic matrices. The methods which determine stability from Eq. 14 are often referred to as *p method* after the non-dimensional complex eigenvalue.

Depending on the nature of the right hand side, Eq. 13 can be solved analytically. In general, however, the aerodynamic force coefficients will be functions of the reduced frequency of oscillation,  $k = fb/u$ , and Mach number and the system needs to be solved iteratively. This procedure is often referred to as the *p-k method* (Hassig (1971)). In this lecture, only steady aerodynamic forces will be considered.

## 2.4 Steady aerodynamic forces

Eq. 13 simplifies significantly if all aerodynamic forces can be calculated from steady state formulas. In this case the angle of attack is assumed to be the instantaneous angle of attack, i.e.  $\theta$ , and there are no aerodynamic loads resulting from the plunging motion. Assuming thin airfoil theory, this results in simple expressions for the aerodynamic force and moment coefficients:  $\tilde{C}_{hh} = \tilde{C}_{\theta h} = 0$  and  $\tilde{C}_{h\theta} = -C_L = -2\pi$  and  $\tilde{C}_{\theta\theta} = -2\pi(a + \frac{1}{2})$ . If these are substituted in Eq. 13, the eigenvalue problem becomes:

$$p^2 \begin{bmatrix} 1 & x_\theta \\ x_\theta & r^2 \end{bmatrix} \begin{bmatrix} \tilde{h}/b \\ \tilde{\theta} \end{bmatrix} + \begin{bmatrix} \frac{\sigma^2}{V^2} & \frac{2}{V^2} \\ 0 & \frac{r^2}{V^2} - \frac{2}{\mu}(a + \frac{1}{2}) \end{bmatrix} \begin{bmatrix} \tilde{h}/b \\ \tilde{\theta} \end{bmatrix} = 0 \quad (15)$$

which can be solved directly for  $p = \lambda b/u$  giving the damping and modal frequency for a given mass ratio, flight velocity and aerofoil geometry. This will be illustrated in Section 3.

## 2.5 Quasi-steady behaviour

In a more sophisticated approximation, *quasi-steady* behaviour is assumed. In this case, the unsteady forces become functions of the instantaneous angle of attack  $\theta$  and its first and second derivatives, as well as the plunge velocity and acceleration:

$$F_{hh} = \pi \rho b^2 \ddot{h} + 2\pi \rho u b \dot{h} \quad (16)$$

$$F_{h\theta} = \pi \rho b^2 [u\dot{\theta} - ba\ddot{\theta}] + 2\pi \rho u b [u\theta + b(0.5 - a)\dot{\theta}] \quad (17)$$

$$F_{\theta h} = \pi \rho b^3 a \ddot{h} + 2\pi \rho u b^2 (a + 0.5) \dot{h} \quad (18)$$

$$F_{\theta\theta} = \pi \rho b^2 [-ub(0.5 - a)\dot{\theta} - b^2(1/8 + a^2)\ddot{\theta}] \quad (19)$$

An explanation of this is out of the scope of this lecture but can be found in Bisplinghoff et al. (2013) (Chapter 5).



### 3 Coupled bending-torsion flutter

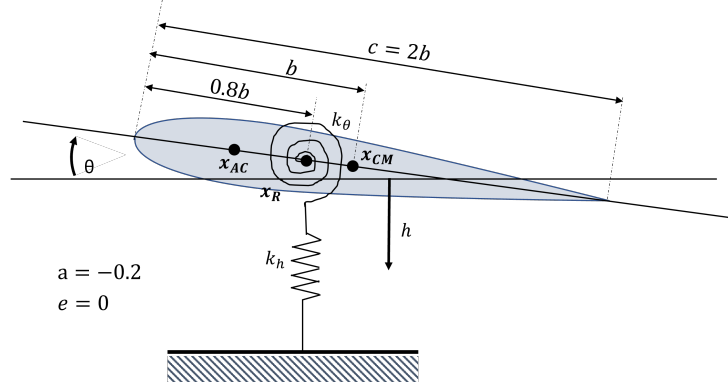


Figure 4: Example typical section with torsional centre located upstream of mid-chord

To demonstrate a typical flutter analysis, we will consider a specific aerofoil section with steady aerodynamic forces as defined above. The aerodynamic centre will be placed at quarter chord, in accordance with thin airfoil theory. Arbitrarily, we will place the centre of mass a little upstream of mid-chord ( $e = -0.1$ ) and the torsional axis further upstream  $a = -0.2$ , as sketched in Fig. 4. We select a mass ratio  $\mu = 20$ , frequency ratio  $\sigma = 0.4$  and radius of gyration  $r^2 = 1/4$ . This results in a radius of gyration around the centre of mass of  $r_{CM}^2 = r^2 - (e - a) = 0.05$ .

In dimensional terms, this might be an aerofoil of chord length 1m with mass per unit span of  $15\text{kg}$  in an air stream of density  $1\text{kg/m}^3$ . If the torsional frequency is  $\omega_\theta = 100\text{Hz}$ , a reduced velocity  $V = 2$  would correspond to a dimensional velocity  $u = 100\text{m/s}$ .

Assuming steady flow, the roots  $p$  of Eq. 15, will define the aeroelastic frequencies  $\omega$  ( $k$  in non-dimensional form) and aerodynamic damping ratio  $\zeta$ :

$$p = \frac{b}{U}(\Gamma + i\Omega) = \frac{b}{U} \left[ \omega\zeta + i\omega\sqrt{1 - \zeta^2} \right] = k\zeta + ik\sqrt{1 - \zeta^2} \quad (20)$$

For  $\zeta \ll 1$ ,  $\omega = \Im(p)U/b$ , and  $\zeta = -\Re(p)/\Im(p)$ . Note that  $k$  here is the inverse of reduced velocity and therefore defined based on semi-chord and frequency in Hz. In literature it is often also defined based on chord length and/or frequency in radians per second.

Figure 5 plots the aeroelastic frequency  $\omega$  normalised by the natural frequency of the twisting motion and the aerodynamic damping ratio  $\zeta$  against the reduced velocity.

As expected, at zero velocity (in absence of aerodynamic forces) there are two independent frequencies corresponding to one dominantly twisting and one dominantly plunging mode. There is a small coupling between these modes because of the off-diagonal terms in the mass matrix, introduced by the off-set of the torsional axis with respect to the centre of mass. At this point, the real part (aerodynamic damping) is necessarily zero. As velocity increases, the two frequencies become closer and at the flutter boundary, when aerodynamic damping becomes negative, the two modes coalesce. This type of instability is called a coupled bending-torsion flutter because the instability is a results of the merging of the two original modes. The roots are now complex conjugate pairs with one having a positive and one a negative real part.

To further demonstrate the nature of this instability, Fig. 6 shows the corresponding eigenvectors which describe the relative magnitude and phase of the plunge and twist displacements at every reduced velocity. For velocities below the flutter velocity  $V < 1.8$  there are two distinct mode shapes, Mode 1, is close to the in-vacuo plunging frequency and the magnitude of the plunge component is much larger than that of the twist. Mode 2 is twist-dominated as expected. As the aerodynamic forces increase, the non-dominant components of each mode grow. At the critical velocity, two coupled modes emerge. For one of them, the twist component is lagging the plunge component while for the other it is leading. This is illustrated in Fig. 7. Mode 1, where the twist component leads the plunge (red lines,  $\phi > 0$ ) is positively damped as seen Fig. 5. For a case 90 degrees, the motion is such that the aerofoil is twisting downwards at the beginning of the downward stroke (max plunge displacement), and upward at the beginning of the upward stroke (see Figure 8). For the other mode (Mode 2) the twist is lagging the plunge component (blue lines,  $\phi < 0$ ). In this case, the aerofoil is twisting upwards at the beginning of the downward stroke and downwards at the beginning of the upward stroke. This is unstable.

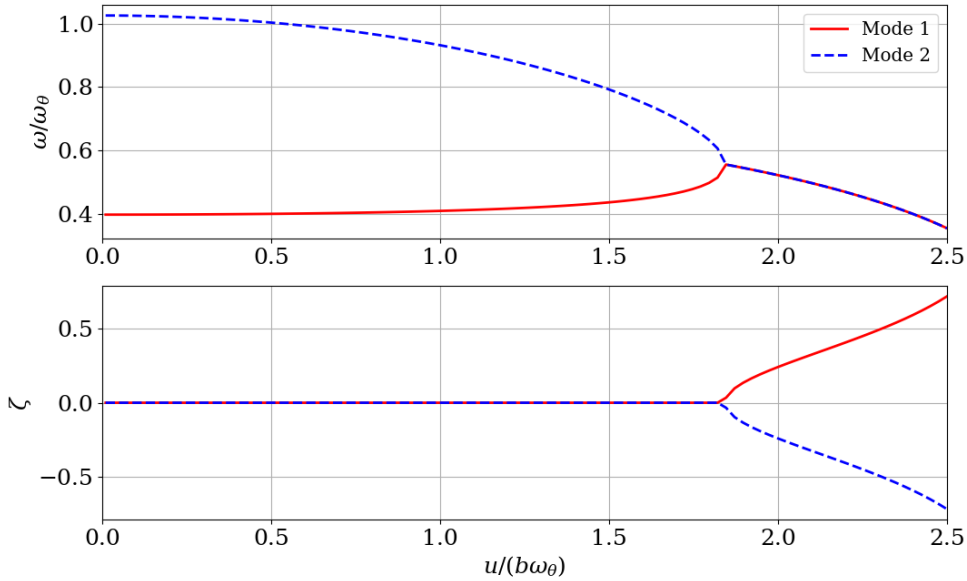


Figure 5: Aeroelastic frequency and aerodynamic damping as a function of reduced velocity for a typical section free to move in plunge and twist

The above analysis has demonstrated how coupled bending-torsion flutter of a typical aerofoil section occurs assuming steady aerodynamic loads. As previously mentioned, this is a radically simplified assumption but it nevertheless provides some insights into the mechanisms of instability (i.e. mode coupling). It can also provide some insights into the importance of the governing non-dimensional parameters, which will be shown in the next section.

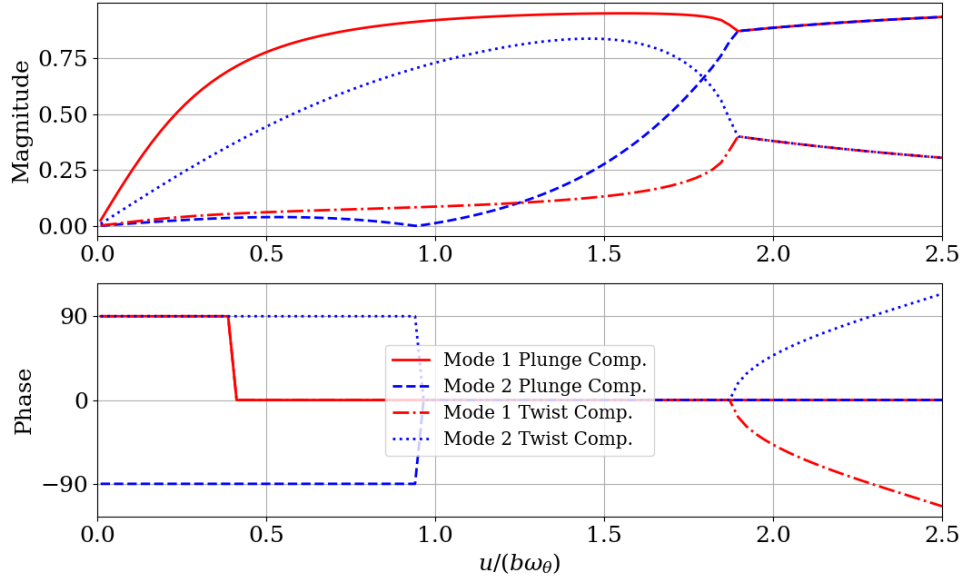


Figure 6: Amplitude and phase of the plunge and twist component in the two aeroelastic modes as a function of reduced velocity

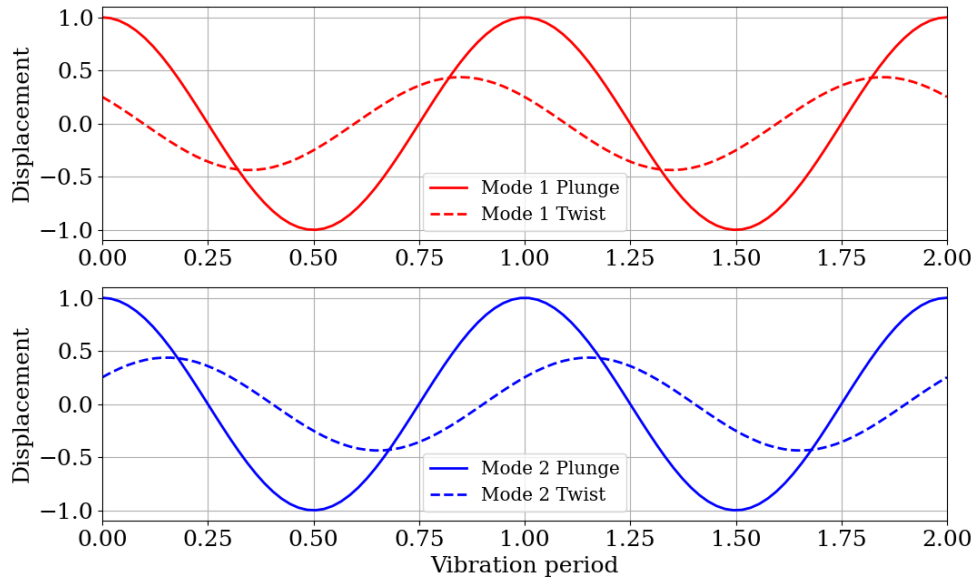
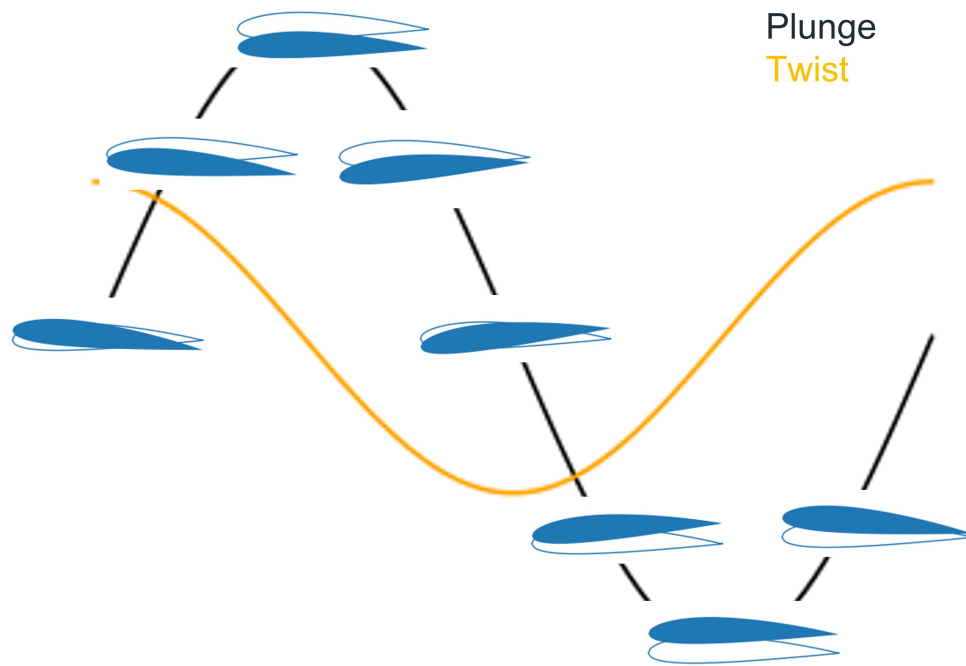
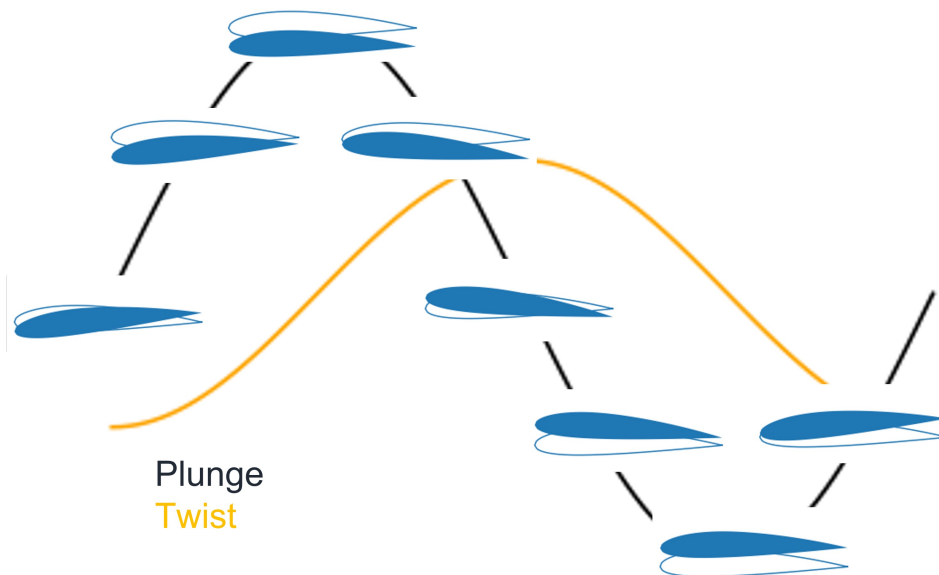


Figure 7: Displacement histories for the plunge and twist component in Mode 1 and Mode 2 at  $V = 2$



(8.1) Twist leading the plunge (stable)



(8.2) Twist lagging the plunge (unstable)

Figure 8: Illustration of unstable and stable twist-plunge motion

## 4 Parameter dependency

The previous section explained flutter instability of an aerofoil cross-section under the influence of steady aerodynamic loads. The instability mechanism was shown to be caused by coupling of the two degrees of freedom (plunge and twist). Despite its simplicity, the typical section demonstrates the important parameters governing stability, which will now be discussed.

From the non-dimensional form of the equation of motion Eq 15, five important parameters can be identified: reduced velocity  $V$ , mass ratio  $\mu$ , frequency ratio  $\sigma$ , torsional axis off-set  $x_\theta = (e - a)$  and the torsional axis location  $a$ . The effect of reduced velocity has already been shown in Fig. 5 and 6. The following will investigate the influence of the three structural parameters on stability.

### 4.1 Mass ratio

The mass ratio is the parameter which scales the aerodynamic forces. Figure 9 shows the aeroelastic frequency for a range of mass ratios for the example shown above. Flutter occurs when the two modes coalesce. It is clear that the flutter speed increases with increasing mass ratio. The higher the mass ratio, the lower is the influence of the aerodynamic forces responsible for mode coupling.

For a given aircraft and speed, mass ratio will change with altitude as air density changes. The fact that low mass ratios are more critical, suggests that the sea level flutter boundary is lower than that at altitude. Furthermore, it shows that coupled bending-torsion flutter is less likely to occur on wings or blades with a high mass per unit span. Light aircraft and gliders with mass ratios  $<15$  are more susceptible to flutter at low reduced velocities. General aviation mass ratios at sea level are approximately 10-20, while helicopter and aero-engine blades can reach 100 (Hodges and Pierce, 2011).

### 4.2 Frequency ratio

The effect of frequency ratio on the aeroelastic eigenvalues is shown in Figure 10. As expected, increasing frequency separation delays the flutter onset. The behaviour is non-linear and flutter velocity drops sharply as the frequency ratio approaches unity. For  $\sigma = 1$  the bending and torsion frequencies would need to be in resonance. This can only occur for unusually high bending stiffness and unusual torsional stiffness, such that this is usually not a concern. It is possible to intentionally design the wing or blade structure to increase the frequency ratio and prevent coupled bending-torsion flutter.

### 4.3 Location of centre of mass and torsional axis

The off-diagonal terms in the mass matrix, i.e. the distance  $x_\theta = (e - a)b$  between the torsional centre and the centre of mass determines the level of structural coupling between the two modes. If  $x_\theta > 0$  the centre of mass lies downstream of the torsional axis as in the example above. If  $x_\theta < 0$  the centre of mass lies upstream of the torsional axis.

Figure 11.1 shows the variation in flutter velocity for an example where the centre of mass is fixed at  $e = 0$  as above, and the location of the torsional centre is varied. At

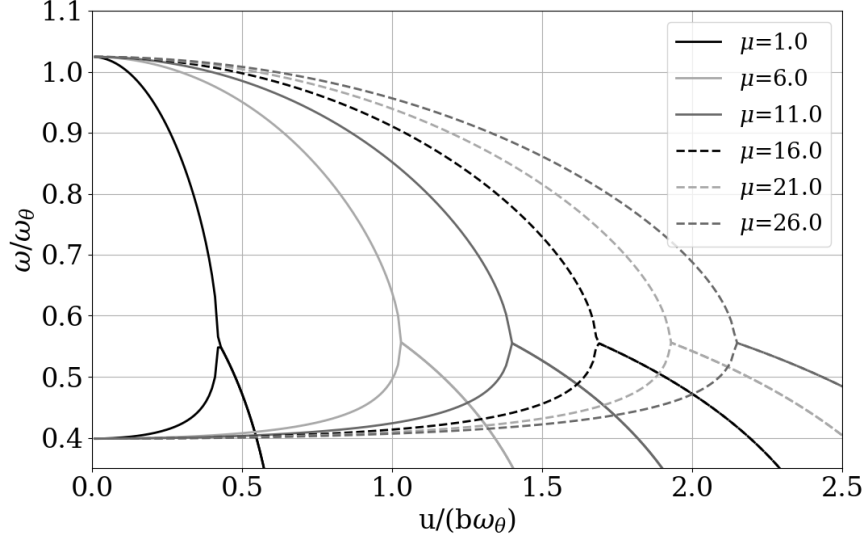


Figure 9: Influence of mass ratio,  $\mu$ , on flutter speed ( $a=-0.2$ ,  $e=-0.1$ ,  $r^2=0.25$ ,  $\sigma=0.4$ )

$a = -0.5$  the torsional centre coincides with the aerodynamic centre at quarter chord, and the matrix becomes singular. As the torsional centre shifts away from the aerodynamic centre, the stability boundary initially moves to lower velocities because the aerodynamic moment induced by the lift force increases, but close to the centre of mass at  $e = 0$ , the flutter speed increases again. There is no more coupling when the centre of mass and aerodynamic centre coincide for this simple example. Similarly, the effect of the static unbalance, i.e. the distance between the centre of mass and the torsional axis, is shown in Figure 11.2 for a fixed torsional axis. A large  $x_\theta$  increases structural coupling between the modes.



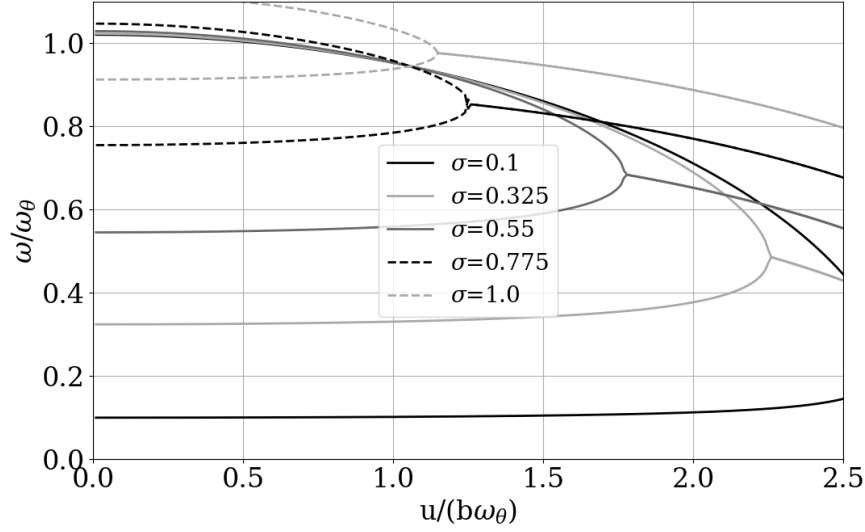
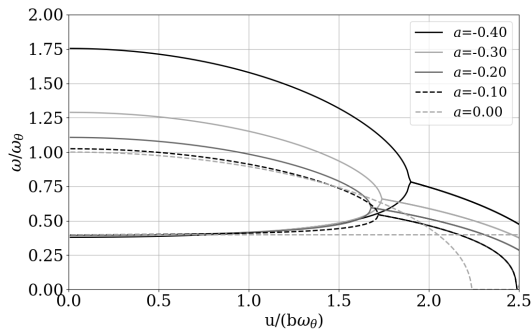
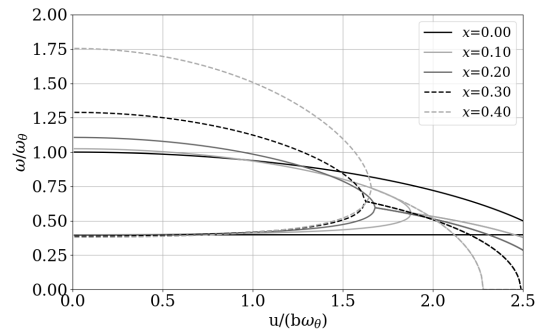


Figure 10: Influence of plunge-twist frequency ratio  $\sigma$  on flutter speed ( $a=-0.2$ ,  $e=-0.1$ ,  $r^2=0.25$ ,  $\mu=25$ )



(11.1) Variation of torsional axis location



(11.2) Variation of static unbalance

Figure 11: Flutter velocity as a function of torsional axis location for a typical section with  $\mu = 20$ ,  $r^2 = 0.25$  and  $\sigma = 0.4$ .



## 5 Conclusions

This lecture has introduced the aeroelastic analysis of a typical aerofoil section with two degrees of freedom: plunging and pitching motion. While the stability analysis, i.e. the formulation and solution of an eigenvalue problem, is general, the results presented here only apply to a typical section with specific structural parameters and assumes steady aerodynamic forces. Nevertheless, a few general conclusions could be drawn:

- Under the influence of aerodynamic forces, the system's dynamics are modified. The aerodynamic forces change the stiffness and introduce damping.
- An instability (negative damping) arises when the bending and torsion modes become coupled under the influence of aerodynamic forces. This occurs at a critical non-dimensional flight speed.
- For coupled bending-torsion flutter with steady aerodynamic forces, the magnitude of the damping depends on the phase-lag between the plunging and twisting motion. If the twisting motion leads the plunging motion, i.e. the aerofoil is pitching upwards at the upward stroke, the system is unstable.
- For a given structure, the flutter speed increases with altitude, such that the critical flutter condition ordinarily arises at sea level.
- A large separation between the natural frequencies of the plunging and torsion mode delays the onset of coupled bending-torsion flutter.

Due to the assumptions made, the instabilities shown in the previous section are limited to coupled bending-torsion instabilities and only occur at low mass ratios, when there is some structural coupling between the modes. In reality, instability conditions are far less restrictive. Flutter in an isolated plunge or twisting mode is possible if there is a phase-lag between the aerodynamic forces and the structural motion, and very high mass ratio structures such as helicopter or turbine blades can also become unstable.

## References

- Bisplinghoff, R. L., Ashley, H., and Halfman, R. L. (2013). *Aeroelasticity*. Courier Corporation.
- Garrick, I. and Reed III, W. H. (1981). Historical development of aircraft flutter. *Journal of Aircraft*, 18(11):897–912.
- Hassig, H. J. (1971). An approximate true damping solution of the flutter equation by determinant iteration. *Journal of Aircraft*, 8(11):885–889.
- Hodges, D. H. and Pierce, G. A. (2011). *Introduction to structural dynamics and aeroelasticity*, volume 15. cambridge university press.

